SUPPLEMENTAL FIGURES

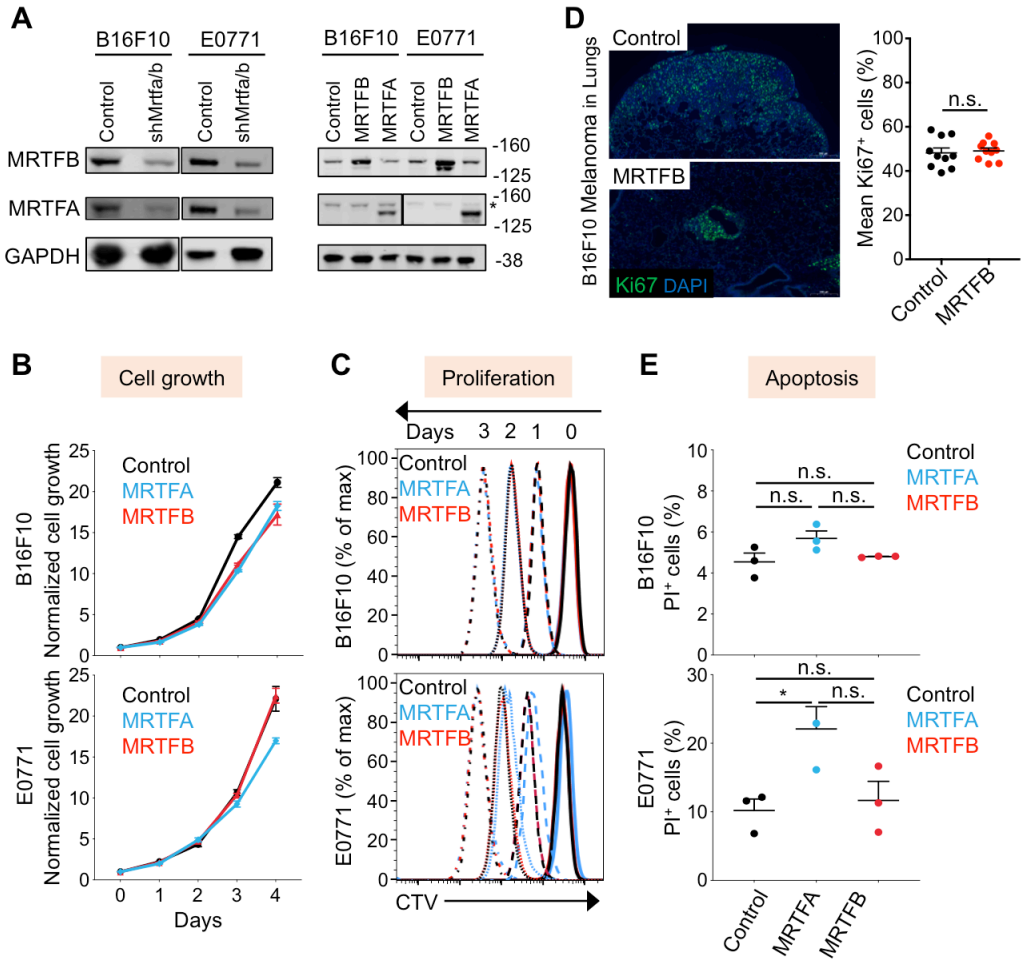

Fig. S1. MRTF does not affect cancer cell growth, proliferation or apoptosis.

Related to Fig. 1. (A) Representative western blots showing MRTFA/B expression levels in the indicated B16F10 and E0771 cell lines. * indicates endogenous MRTFA. (B) Cellular growth kinetics of the indicated B16F10 (above) and E0771 (below) cell lines, measured by CellTiterGlo normalized to first day of plating (Day 0). Error bars: SEM. *n* = 3 technical replicates. Results are representative of two independent experiments. (C) Cellular proliferation measured by CTV (Cell Trace Violet) dilution, after CTV staining on day 0. Data are representative of 3 independent experiments. (D) Left, immunofluorescence images showing proliferative state (Ki67, green) of B16F10 melanoma cells expressing control vector or MRTFB during lung colonization of syngeneic mice. DAPI, nuclear stain, blue. Right, quantification of Ki67 staining, with data shown as mean ± SEM, n.s.: not significant for $p > 0.05$; two-tailed unpaired Student's t test (*n* = 10 mice per group). (E) Graphs showing the percentage of cell

apoptosis quantified by propidium iodide (PI) incorporation. Data from 3 independent experiments shown as mean ± SEM (One-way ANOVA with Tukey's multiple comparisons test; n.s.: not significant for $p > 0.05$, $*p \leq 0.05$).

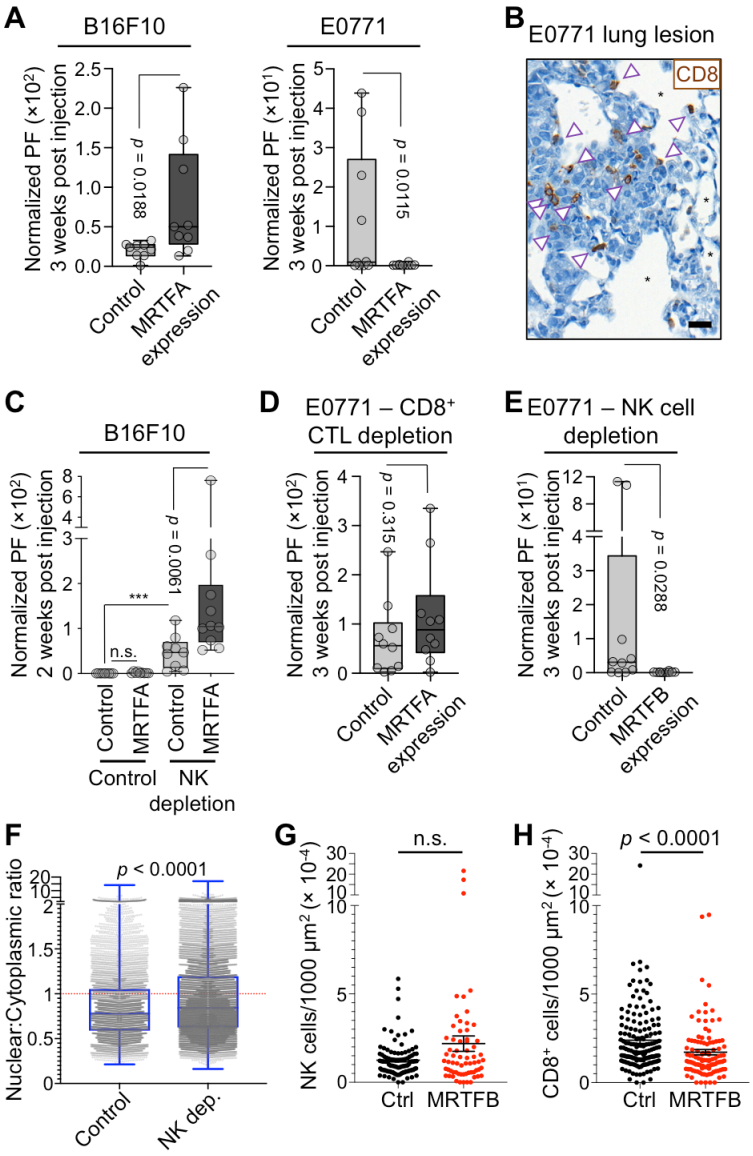

Fig. S2. Immune vulnerability of cancer cells during metastatic colonization.

Related to Fig. 1. (A) BLI of mouse lungs 3 weeks post tail vein injection with B16F10 melanoma (left) or E0771 breast cancer (right) cells overexpressing empty vector or MRTFA (n = 9 mice per group). (B) Representative IHC images of $CD8^+$ T cell (brown arrowheads, CD8 staining) infiltration in E0771 breast cancer lung metastases. *: alveolar space, Scale bar: 20 µm. (C) BLI of mouse lungs 2 weeks after tail vein injection with B16F10 cells with or without NK cell depletion using anti-Asialo GM1 antibody, showing sensitivity of MRTFA overexpressing cells to NK cells during lung colonization. n.s. :not significant, p = 0.077, ****p < 0.0001 (n = 10 mice for MRTFA, NK cell depletion and n = 9 mice for others). (D-E) BLI of mice pretreated with anti-CD8 antibody (D) or anti-asialo GM1 antibody (E) for T and NK cell depletion, respectively, and imaged 3

weeks after injection of indicated cancer cells (n = 10 mice per group). (F) B16F10 lung metastases from control and anti-asialo GM1 treated (NK cell depletion) mice were stained for MRTFB. Nuclear accumulation of MRTFB in B16F10 tumor cells (for each column, $n \geq 7780$ cells, from ≥ 3 mice). (G-H) Quantification of NK cell (G) and $CD8^+$ T cell (H) density in sections derived from control B16F10 (black) and B16F10-MRTFB (red) metastases. Error bars denote mean ± SEM (for each column, $n \geq 99$ lesions, taken from ≥ 3 mice). Throughout figure, box plots show upper and lower quartiles, median, maximum, and minimum values. All p values were calculated by Mann-Whitney test.

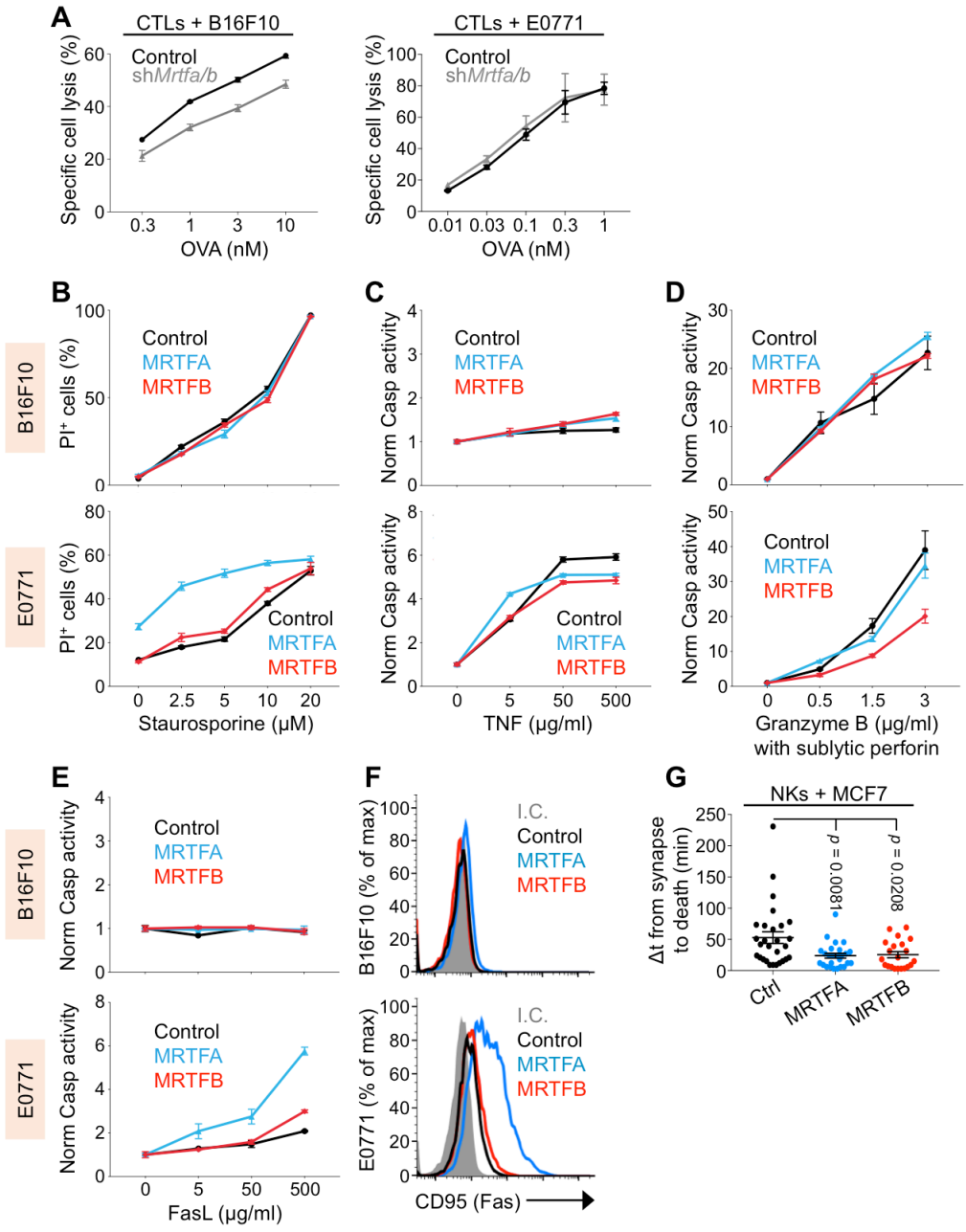

Fig. S3. Effects of MRTF expression on cellular cytotoxicity and other forms of cell death.

Related to Fig. 2. (A) Specific lysis of control or *Mrtfa/b* knockdown B16F10 (left) or E0771 (right) cells 5 h after mixing with CTLs. (B-E) B16F10 (top) and E0771 (bottom) control and MRTFA or MRTFB overexpressing cell lines were treated with the indicated concentrations of staurosporine (B), TNF (C), granzyme B plus a sublytic concentration of perforin (D), or FasL (E) and cell apoptosis was quantified by propidium iodide (PI) incorporation (B) or the caspase Glo 3/7 assay system after normalization to each cell

line's untreated samples (C-E). Data in A-E shown as mean ± SEM of technical triplicates, representative of at least 2 independent experiments. (F) Flow cytometric analysis of Fas on the indicated control and MRTFA/B overexpressing cell lines. Isotype control (I.C.) is shown in gray. Histograms are representative of 3 independent experiments. (G) Human NK cells labeled with cell trace violet were imaged together with Calcein Red-Orange-labeled MCF7, MCF7-MRTFA, or MCF7-MRTFB cells. Graph shows the time delay between synapse formation and death (Calcein Red-Orange leakage), quantified for 1:1 synapses ($n \geq 21$ conjugates for each group). Error bars denote mean ± SEM. *p* values were calculated by Mann-Whitney test. Data pooled from 3 independent experiments.

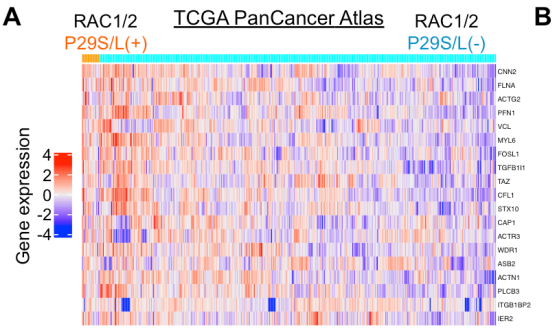

B

TCGA	Number of Cases, Total	Number of Cases, Deceased	Median Months Survival
RAC1/2 P29S/L (+)	18	11	49.51
RAC1/2 P29S/L (-)	330	172	98.40

Anti-PD1/ PDL1	Number of Cases, Total	Number of Cases, Deceased	Median Months Survival
RAC1/2 P29S/L (+)	11	3	32.5
RAC1/2 P29S/L (-)	364	91	68.2

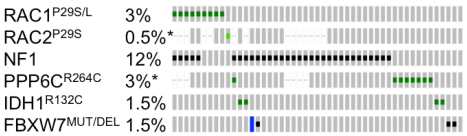

D

Anti-CTLA4	Number of Cases, Total	Number of Cases, Deceased	Median Months Survival	Survival *p-value* in anti-CTLA4	Normalized SRF Gene Enrichment Score	SRF GSEA *q-value* in TCGA
RAC1/2 P29S/L (+)	10	2	NA	**0.0297**	1.81	**0.026**
RAC1/2 P29S/L (-)	263	157	26.68			
NF1 Truncation (+)	32	14	96.50	0.0712	1.24	0.232
NF1 Truncation (+) RAC1/2 P29S/L (-)	27	13	31.32	0.227		
NF1 Truncation (-)	241	145	25.00			
PPP6C R264C (+)	8	6	7.37	0.0881	0.21	0.813
PPPC R264C (-)	265	153	28.62			
IDH1 R132C/L (+)	4	1	31.32	0.294	-1.26	0.201
IDH1 R132C/L (-)	269	158	28.00			
FBXW7 Mut (+)	4	4	9.93	0.273	1.36	0.153
FBXW7 Mut (-)	269	155	28.62			

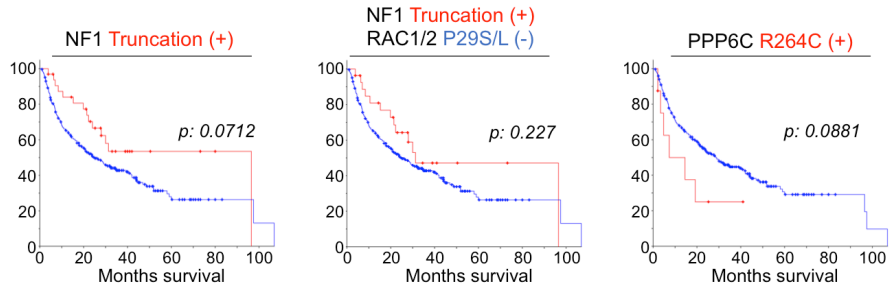

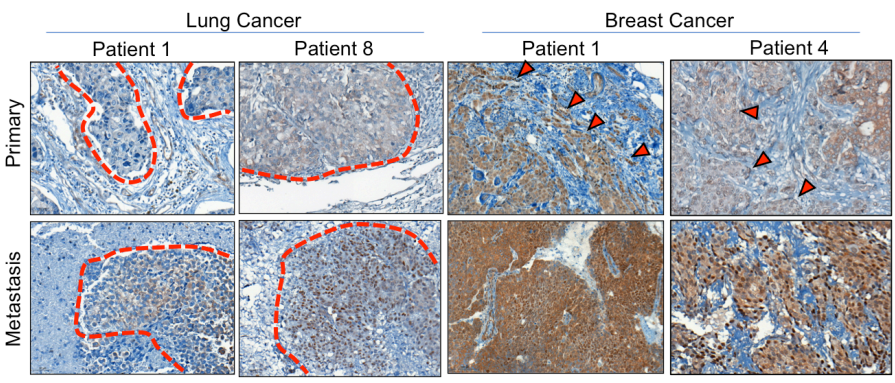

Fig. S4. An MRTF-SRF gene signature correlates with responsiveness to ICB.

Related to Fig. 3. (A) Heat map representation of differential gene expression Z-scores for the leading genes in the MRTF-SRF gene signature applied to the TCGA PanCancer Atlas skin cutaneous melanoma dataset. (B) Total number of patients, RAC1/2 mutational status, vital status, and median survival in months for the TCGA skin cutaneous melanoma data set (above) and the anti-PD1/PDL1 MSK-IMPACT data set (below). (C) Oncoprint showing the overlap between distinct sets of mutations in patients from the anti-CTLA4 cohort analyzed in Fig. 3I. Each grey bar is a profiled patient, with dashes representing no available data on a particular gene. The frequency of each mutation is indicated as a percentage. Color-coding on each bar represents a mutation or a genomic alteration annotated as oncogenic by oncoKB. Green and black squares are oncogenic driver point mutations and truncations, respectively. Blue bars denote deep genomic deletions. n = 273 patients. * indicates that not all patients were profiled for the queried genomic event. Patients with no alterations were included in the analyses but were cropped from the panel for simplicity. (D) Survival statistics for mutations depicted in C. The first four columns contain statistics from the anti-CTLA4 cohort, while the last two columns of SRF signature statistics are derived from the TCGA skin cutaneous melanoma cohort. Bolded values are statistically significant. (E) Kaplan-Meier curves showing overall survival of melanoma patients from the anti-CTLA4 cohort bearing the indicated UV-induced mutations. *p* values were calculated by Log-rank test. (F) Representative images of immunohistochemical staining of MRTFB in primary lung and breast cancer tumors along with matched brain metastases (*n* = 4 and 7 lung and breast cancer patients, respectively). Red lines outline lung cancer cells. Red triangles indicate strong nuclear MRTFB staining in the breast cancer cells.

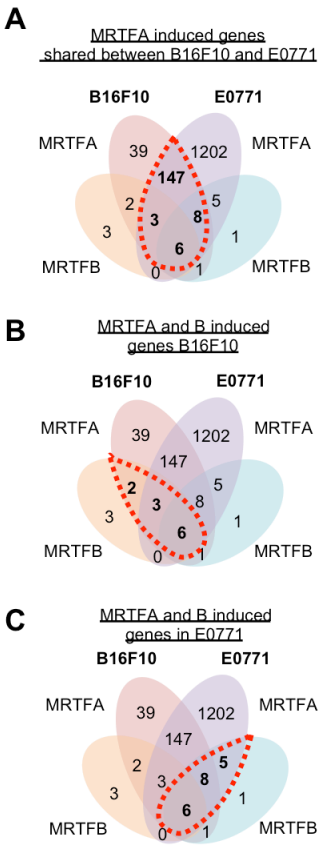

Gene Ontology: Biological Process		
Term	*P-value*	Fold Enrichment
actin cytoskeleton organization	7.98E-06	5.0
myofibril assembly	6.55E-06	21.0
striated muscle cell development	1.46E-05	10.0
muscle cell development	3.09E-05	9.0
striated muscle cell differentiation	6.02E-05	6.5
actin filament organization	5.06E-05	5.9
muscle cell differentiation	9.38E-05	5.1
actomyosin structure organization	4.72E-04	8.5
mesenchyme migration	6.23E-04	106.4
striated muscle contraction	2.02E-03	8.1

Gene Ontology: Biological Process		
Term	*p* value	Fold Enrichment
mesenchyme migration	3.02E-08	1960.2
mesenchyme morphogenesis	3.13E-05	192.2
skeletal myofibril assembly	1.55E-04	816.8
mesenchyme development	1.79E-03	39.8
myofibril assembly	4.09E-03	129.0
actomyosin structure organization	2.55E-02	46.8
striated muscle cell development	2.27E-02	45.9
muscle cell development	2.43E-02	41.5

Gene Ontology: Biological Process		
Term	*p* value	Fold Enrichment
mesenchyme migration	3.85E-03	643.2

Fig. S5. RNA sequencing analysis of MRTFA and MRTFB expressing cells.

Related to Fig. 4. (A-C) Left, Venn diagrams of MRTF-induced genes exclusive to or shared by B16F10 and E0771 cells, with bold numbers and red dashed circles highlighting gene sets used for the GO analyses on the right. Up to 10 statistically significant GO terms are shown in each table, with reported *p* values corrected for multiple testing using the Benjamini method.

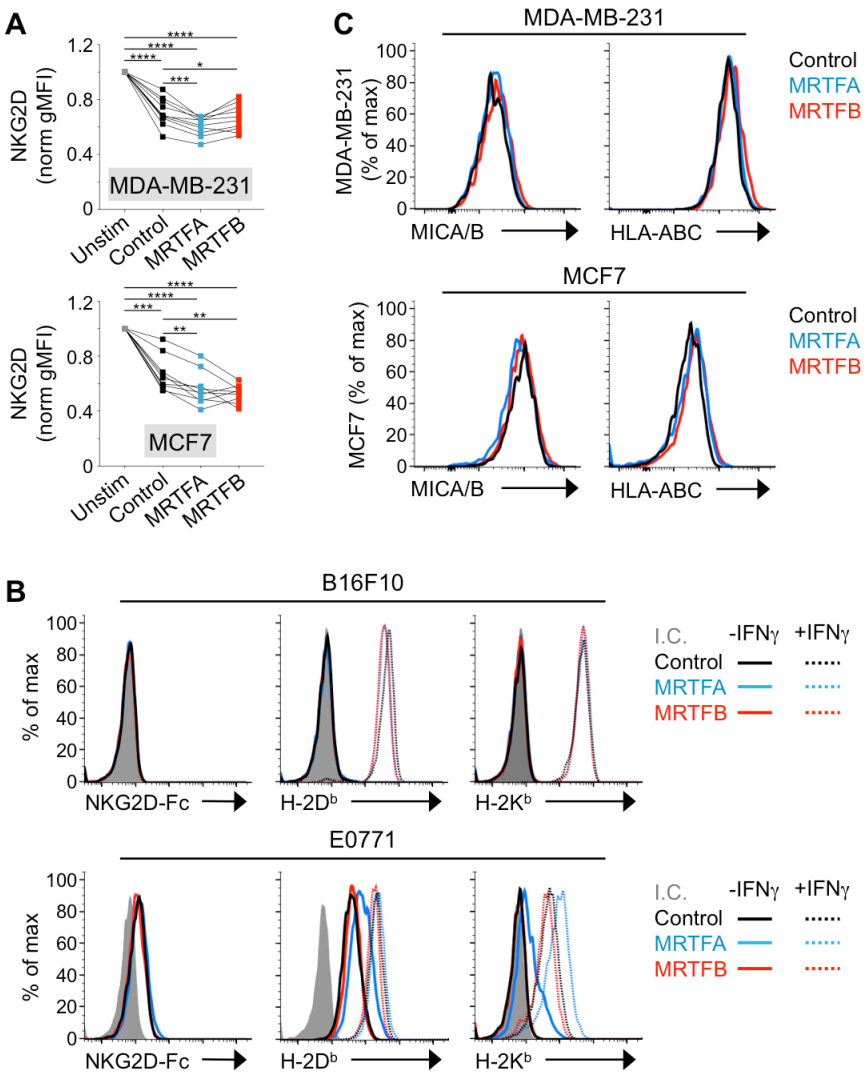

Fig. S6. Surface protein expression on cells overexpressing MRTFA or MRTFB. Related to Fig. 6 and Fig. 7. (A) Flow cytometric analysis of NKG2D expression on human NK cells after 5 h coculture with the indicated target cells. Data were normalized against NKG2D levels on untreated NK cells. Gray lines indicate samples derived from the same donor. ****$p < 0.0001$, ***$p < 0.001$, **$p < 0.01$, and *$p < 0.05$ calculated by one-way ANOVA (n = 9 donors for MCF7 experiments, n = 10 donors for MDA-MB-231 experiments). Data pooled from 3 independent experiments. (B) Flow cytometric analysis of NKG2D ligands and MHC proteins (H2Db and H2Kb) on the indicated control or MRTFA/B overexpressing B16F10 and E0771 cell lines. Cells were untreated (solid lines) or pretreated overnight with IFNγ (dotted lines). Isotype control (I.C.) is shown in gray. Histograms are representative of 3 independent experiments. (C) Flow cytometric analysis of MICA/B (NKG2D ligands) and HLA-ABC (MHC) on the indicated control and

MRTFA/B overexpressing MDA-MB-231 and MCF7 cell lines. Histograms are representative of 3 independent experiments.

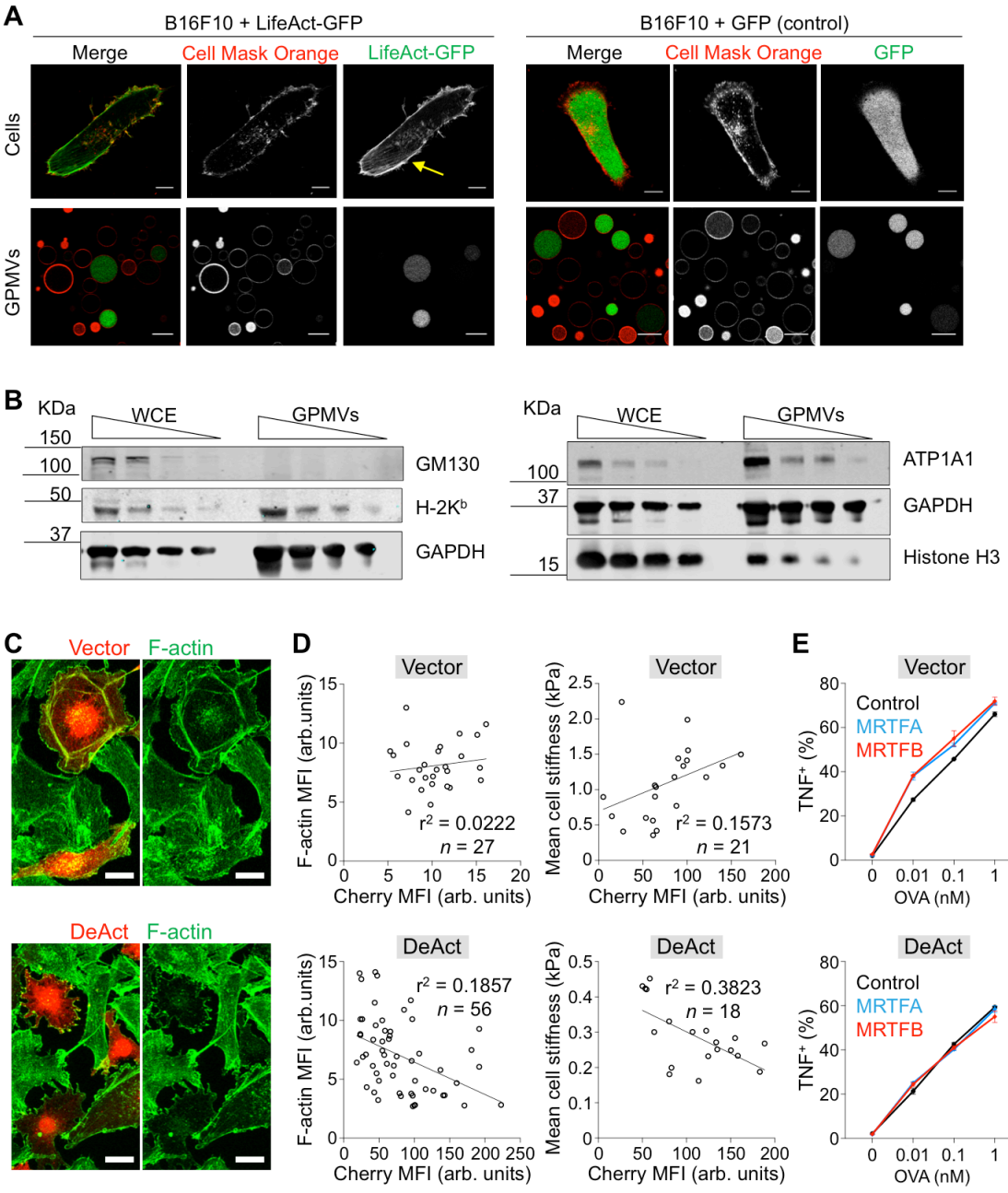

Fig. S7. Characterization of giant plasma membrane vesicles (GPMVs) and DeAct. Related to Fig. 6 and 7. (A) Representative confocal images of whole cells (above) and cell-derived GPMVs (below). B16F10 cells overexpressing LifeAct-GFP (green, left panel) or GFP control (green, right panel) were labeled with the plasma membrane dye Cell Mask Orange (red). The yellow arrow indicates cortical F-actin present in cells but not in GPMVs. Scale bars: 10 μm. (B) Immunoblots of the indicated proteins, performed using serial dilutions of whole cell extracts (WCE) or GPMVs derived from B16F10 cells. GADPH served as a loading control. (C) Representative confocal images of B16F10

cells transfected with DeAct or Cherry control vector, fixed and stained for F-actin (phalloidin). Transfected cells were identified by coexpression of Cherry. Scale bars = 10 µm. (D) Scatterplots correlating transfection efficiency of DeAct or control vector (evaluated by Cherry expression) with either F-actin MFI (left, evaluated by confocal image analysis) or cell stiffness (evaluated by AFM). Trend lines were derived by linear regression. (E) B16F10 cells overexpressing MRTFA, MRTFB, or empty vector were transfected with DeAct (bottom) or vector control (top), loaded with increasing concentrations of OVA, and then mixed with OT1 CTLs. TNF production was measured after 4 h. Data are shown as mean ± SEM of technical triplicates. Data are representative of at least 2 independent experiments.